Supplementary Information (SI) for Journal of Materials Chemistry A.
This journal is © The Royal Society of Chemistry 2026

Supplementary Information

Interface-Engineered Graphene Oxide Membranes for High-Performance Fluorine-Free Fuel Cells

Tatsuki Tsugawa,[a] Kazuto Hatakeyama,*[b] Kanako Oka,[a] Kaito Takegami,[a] Yuichi Sakuda,[b] Michio Koinuma [b] and Shintaro Ida*[b]

Affiliations:

[a] Institute of Industrial Nanomaterials (IINa), Kumamoto University; 2-39-1 Kurokami, Chuo-ku, Kumamoto 860-8555, Japan.

[b] Graduate School of Science and Technology, Kumamoto University; 2-39-1 Kurokami, Chuo-ku, Kumamoto 860-8555, Japan.

*Corresponding authors Email: hatakeyama-k@kumamoto-u.ac.jp, ida-s@kumamoto-u.ac.jp

Methods

Synthesis of GO Nanosheets

H-GO was synthesized via the modified Hummers' method.[37] In an ice bath, 2 g of graphite powder was mixed with 2 g of $NaNO_3$ (FUJIFILM Wako Pure Chemical Corporation) and 92 mL of concentrated H_2SO_4 (FUJIFILM Wako Pure Chemical Corporation) under continuous stirring. Subsequently, 10 g of $KMnO_4$ (FUJIFILM Wako Pure Chemical Corporation) was added gradually. After addition, the mixture was slowly diluted with water, followed by the addition of 5 mL of H_2O_2 solution (FUJIFILM Wako Pure Chemical Corporation) to terminate the reaction. The resulting suspension was centrifuged at 3000 rpm, and the supernatant was discarded. The precipitate was washed sequentially with 5% HCl solution and deionized water. The oxidized graphite was then dried in an oven at 50 °C. The dried product was dispersed in deionized water at a 1:1 weight ratio and exfoliated by ultrasonication for 2 h. After centrifugation at 8000 rpm, the supernatant containing monolayer nanosheets was collected, while the precipitate was washed three times with water at 15000 rpm to obtain the H-GO dispersion.

For comparison, B-GO nanosheets were synthesized using a modified Brodie's method.[38] 1 g of graphite powder (FUJIFILM Wako Pure Chemical Corporation) was mixed with 40 mL of fuming HNO_3 (FUJIFILM Wako Pure Chemical Corporation) and stirred in an ice bath. Then, 8 g of $KClO_3$ (FUJIFILM Wako Pure Chemical Corporation) was added slowly, and the mixture was stirred at room temperature for 1 h. The suspension was washed with deionized water, and the precipitate was separated by centrifugation at 3000 rpm. The oxidized graphite was dried in an oven at 50 °C. Subsequently, 500 mg of the dried oxidized graphite was added to 500 mL of ammonia solution (pH 12.5), shaken for 5 days, and exfoliated by ultrasonication for 30 min. Unexfoliated graphite oxide was removed by centrifugation at 3000 rpm, and the supernatant was collected at 8000 rpm. Finally, the nanosheets were precipitated by high-speed centrifugation at 15000 rpm, washed three times with deionized water, and redispersed to obtain B-GO.

Preparation of GO Membranes

Self-standing GO membranes for proton conductivity measurement and fuel cell characterization were prepared by vacuum filtration. A filter holder (KG-47, ADVANTECH) and an aspirator (A-1000S, EYELA) were employed, using an inorganic Anodisk membrane (diameter 47 mm, pore size 0.2 μm) as the support substrate.

Proton Conductivity Measurement

Out-of-plane proton conductivity of the GO membranes was evaluated using both mirror-polished electrodes (area: 0.745 cm^2) and porous electrodes (area: 0.1256 cm^2). For measurements with the dies, the samples were placed in an environmentally controlled chamber at 25 °C and 100%

RH for 1 h. In the fuel cell setup, argon gas was continuously supplied and bubbled through water before entering the cell to maintain humidification. Impedance spectra (Nyquist plots) were recorded using an IviumStat.h potentiostat (Ivium Technologies) with a perturbation voltage amplitude of 100 mV over a frequency range of 1 MHz to 0.1 Hz. Proton conductivity (σ) was calculated using the equation (1):

$$\sigma = \frac{T}{(R \times S)} \quad (1)$$

where T is the thickness of the GO membrane, R is the proton conductivity resistance (Ω) obtained by fitting the Nyquist plot using the equivalent circuit shown in Figure S5, and S is the electrode area. Temperature control during the measurements was maintained using a thermostatic chamber at (25–40 °C).

Fuel Cell Performance Tests

Fuel cell performance was evaluated using a single-cell test holder (Pem Master PEM-004; Chemix) as shown in Figure S13a. Commercial carbon paper coated with a Pt/C catalyst layer (Chemix) was used as both the anode and cathode. Performance measurements were recorded and corrected using a potentiostat equipped with a function generator (Hokuto Denko). The cell temperature was maintained at 25–40 °C in a thermostatic chamber. Wet hydrogen (H_2, 100% RH) and oxygen (O_2, 100% RH) gases were supplied to the anode and cathode, respectively. Protonic interfacial modification was performed by dropping an aqueous MSA solution onto the membrane surface and allowing short-time immersion prior to fuel cell assembly, followed by transferring the GO membrane onto a Pt-supported carbon electrode (Pt: 2.0 mg cm^{-2}) using the blotting method. After the treatment, excess residual MSA was removed by aspiration using a dropper. For durability evaluation, both OCV monitoring and constant-voltage tests were conducted. In the constant-voltage test, a potential of 0.6 V was continuously applied via chronoamperometry, and the resulting current was monitored over time.

Measurement of the concentration cell employing water vapor

A schematic diagram of the water vapor concentration cell is shown in Figure S16a. EMF measurements were performed using a fuel cell test cell O_2 gas flow. The EMF was recorded using a potentiostat equipped with a function generator (Hokuto Denko). Temperature was maintained at 25 °C in a thermostatic chamber.

For a proton-conducting membrane, the reactions at each electrode are as follows:

- Wet side: $2H_2O \rightarrow O_2 + 4H^+ + 4e^-$
- Dry side: $4H^+ + O_2 + 4e^- \rightarrow 2H_2O$

The proton transport number t_H was estimated using a water vapor concentration cell and the following

Nernst equation (2):

$$EMF = -t_H \frac{RT}{2F} \ln \frac{PH_2O^{II}}{PH_2O^{I}} \quad (2)$$

where R is the gas constant (8.31 J K^{-1} mol^{-1}), T is the absolute temperature (K), F is the Faraday constant (96500 C mol^{-1}), PH_2O^{I} (= 100% RH) and PH_2O^{II} (= 10, 20, 30% RH) are the water vapor partial pressures, respectively.

Characterization

The morphology of GO nanosheets was observed using atomic force microscopy (AFM, Nanocute; Hitachi High-Technologies). AFM samples were prepared by dropping a GO aqueous dispersion onto mica substrates and subsequently drying. Transmission electron microscopy (TEM, JEM-ARM200F NEOARM, JEOL) was conducted at an acceleration voltage of 60 kV. The cross-sectional morphology and elemental distribution of thick GO membranes were analyzed using scanning electron microscopy (SEM, SU-8000; Hitachi High-Technologies) coupled with energy-dispersive X-ray spectroscopy (SEM-EDS). Cross-sectional MEA samples were prepared by an ion milling system (E-3500; Hitachi High-Technologies). The overall elemental composition of the samples was determined by CHN analysis for carbon, hydrogen, and nitrogen, and by quantitative sulfur analysis (S analysis). The microscale elemental distribution was further conducted using electron probe microanalysis (EPMA; EPMA-1720H, Shimadzu Corporation), enabling evaluation of both the bulk composition and local elemental distribution. Fourier-transform infrared (FT-IR, Nicolet iS50, Thermo Fisher Scientific) spectra were recorded in attenuated total reflection (ATR) mode at room temperature and ambient pressure. Surface elemental composition was further investigated by X-ray photoelectron spectroscopy (XPS, GENESIS, PHI Corporation). The C 1s spectrum was deconvoluted into five peaks corresponding to O=C–OH (288.8 eV), C=O (287.8 eV), C–O–C (287.1 eV), C–OH (286.4 eV), and C–C (285.0 eV). Out-of-plane X-ray diffraction (XRD, SmartLab; Rigaku) was performed using Cu Kα radiation (λ = 0.154 nm). For XRD measurements, GO membranes were prepared by drop-casting an aqueous GO dispersion onto glass substrates and drying in an oven at 50 °C.

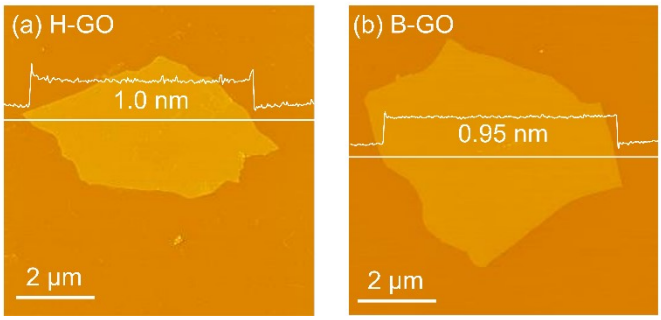

Figure S1. AFM images of (a) H-GO and (b) B-GO nanosheets.

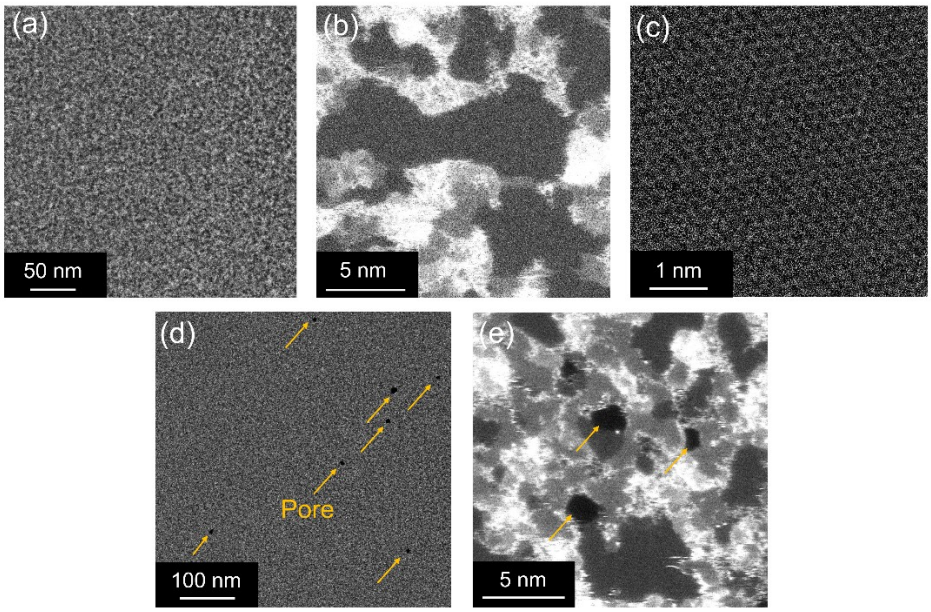

Figure S2. Structural characterization of B-GO and H-GO. HAADF-STEM images of B-GO with (a) low, (b) medium, and (c) high magnifications, and of H-GO with (d) low and (e) high magnifications.

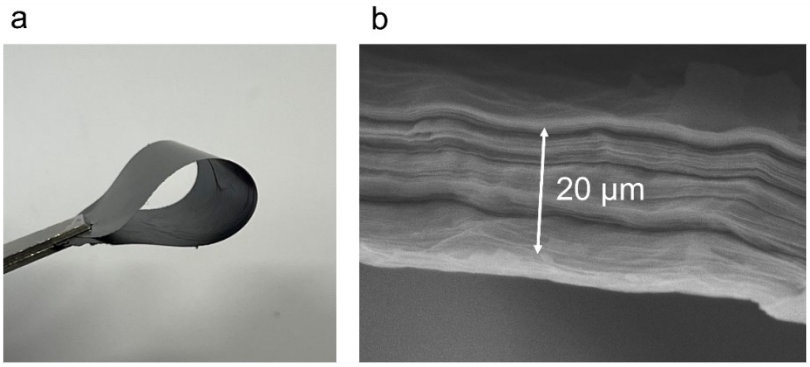

Figure S3. (a) Optical photograph of H-GO membrane. (b) Cross-sectional SEM image of GO membrane.

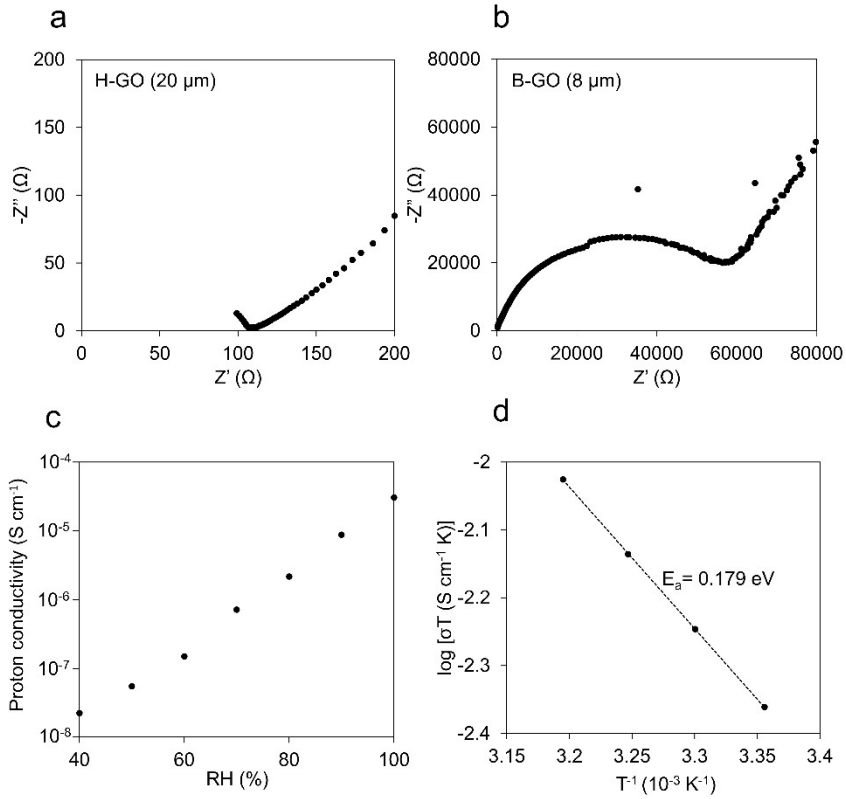

Figure S4. Impedance spectra for out-of-plane proton conductivity of (a) H-GO and (b) B-GO membranes. (c) Humidity dependence of out-of-plane proton conductivity in the H-GO membrane at 25 °C. (d) Arrhenius plot of out-of-plane proton conductivity for the H-GO membrane at 100% RH. E_a is the activation energy.

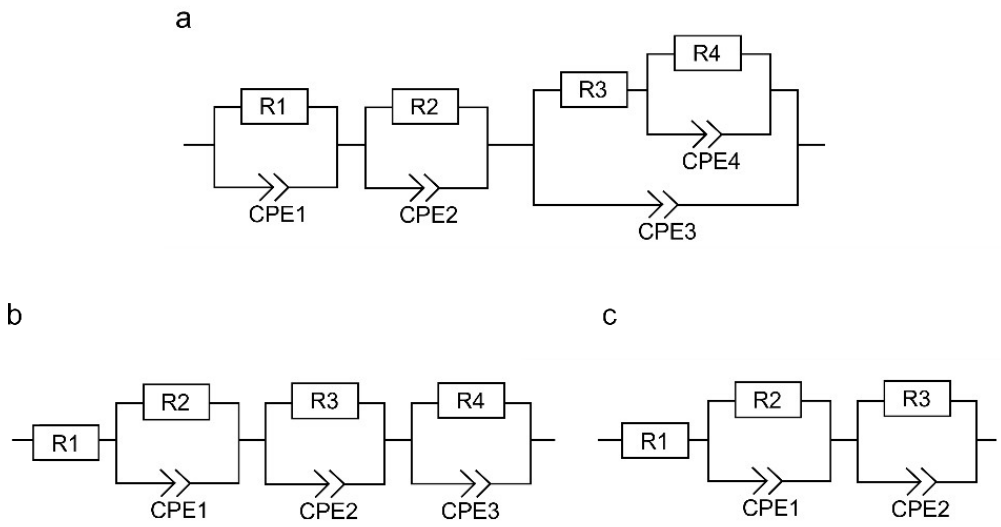

Figure S5. Equivalent circuit models used for fitting Nyquist plots corresponding to Figure 2(a)–(c).

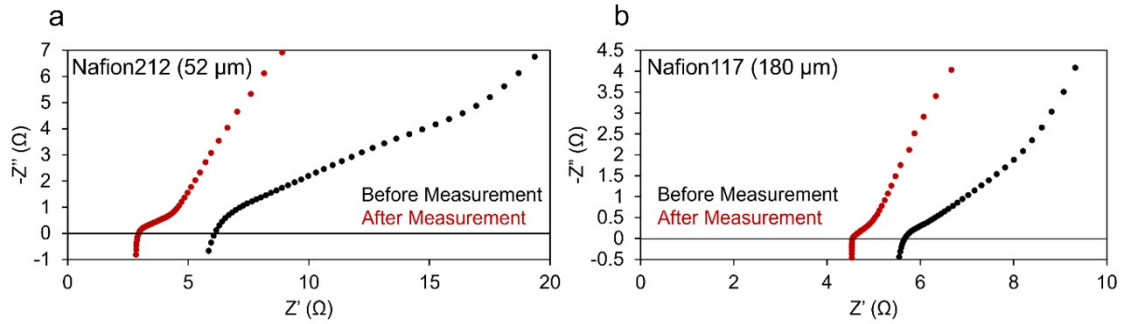

Figure S6. Impedance spectra of (a) Nafion 212 (52 µm) and (b) Nafion 117 (180 µm) membranes. Black and red dots represent measurements before and after fuel cell measurements, respectively.

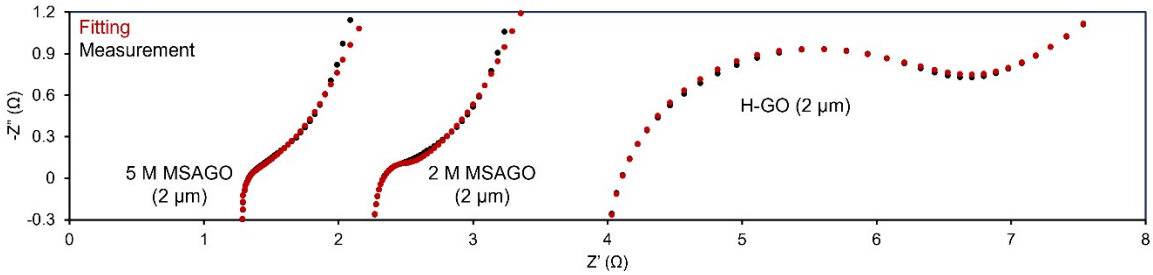

Figure S7. The Nyquist plots of 2 μm H-GO, 2 M MSAGO, and 5 M MSAGO membranes after fuel cell evaluation.

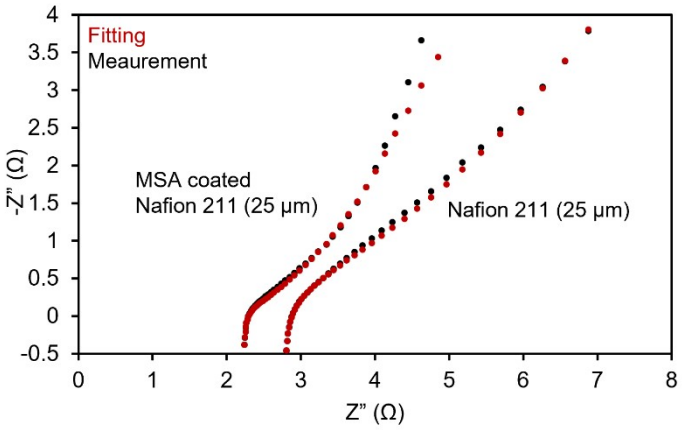

Figure S8. The Nyquist plots of 2 µm H-GO, 2 M MSAGO, and 5 M MSAGO membranes after fuel cell evaluation.

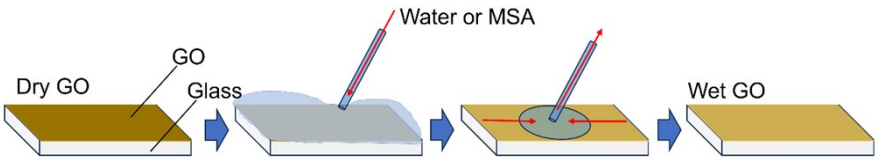

Figure S9. Preparation procedure of wet GO membranes for XRD measurements. Water and MSA were dropped onto the membrane surface, excess MSA was removed by washing with water, and the membrane was subsequently dried.

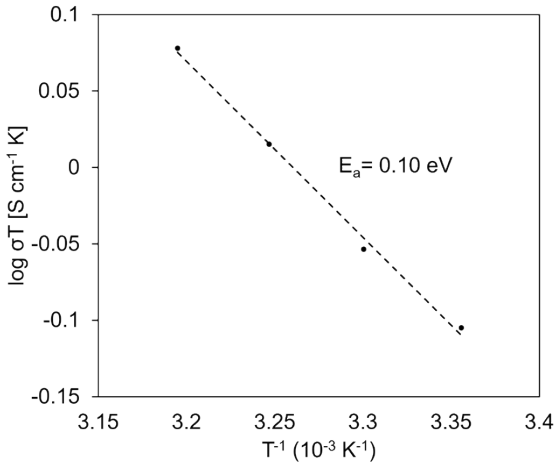

Figure S10. Arrhenius plot of out-of-plane proton conductivity for the MSAGO membrane at 100% RH. E_a is the activation energy.

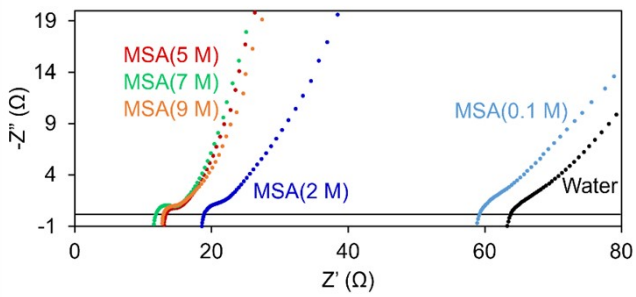

Figure S11. MSA concentration dependence in the impedance spectra of MSAGO membranes.

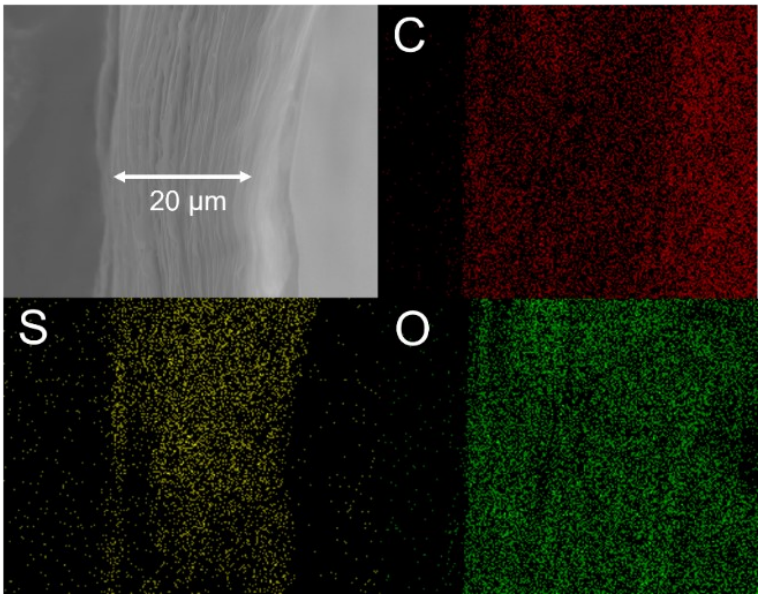

Figure S12. Cross-sectional SEM images and SEM-EDS elemental mapping of MSAGO membrane.

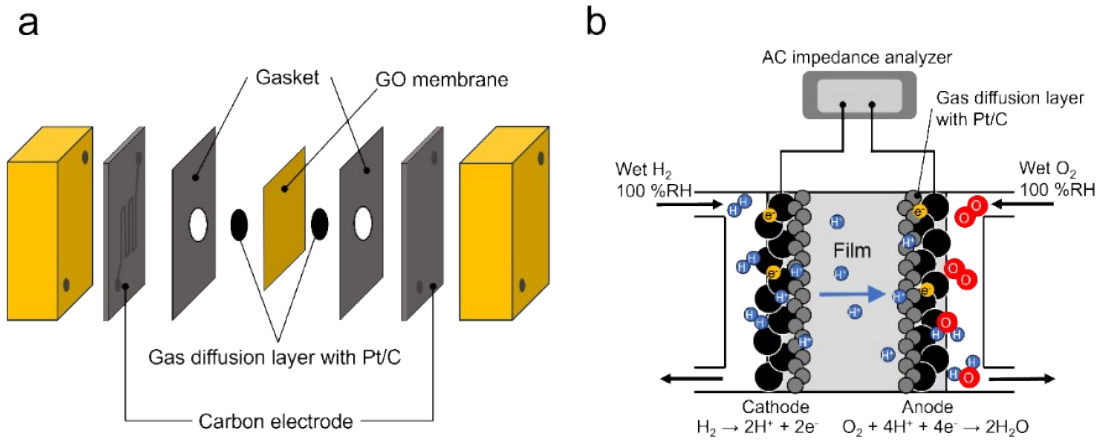

Figure S13. (a) Configuration diagram of the single fuel cell. (b) Schematic diagram of reaction in the system of (a).

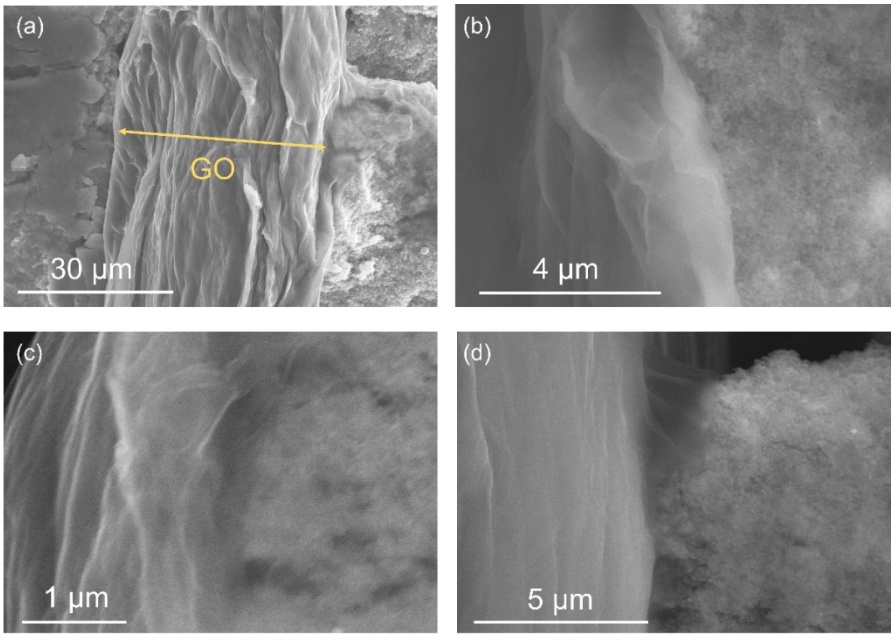

Figure S14. (a) Cross-sectional SEM image of GO MEA after MSA coating, sandwiched between commercially available electrodes with catalyst layers. (b)–(d) High-magnification images views of the electrode–electrolyte interface.

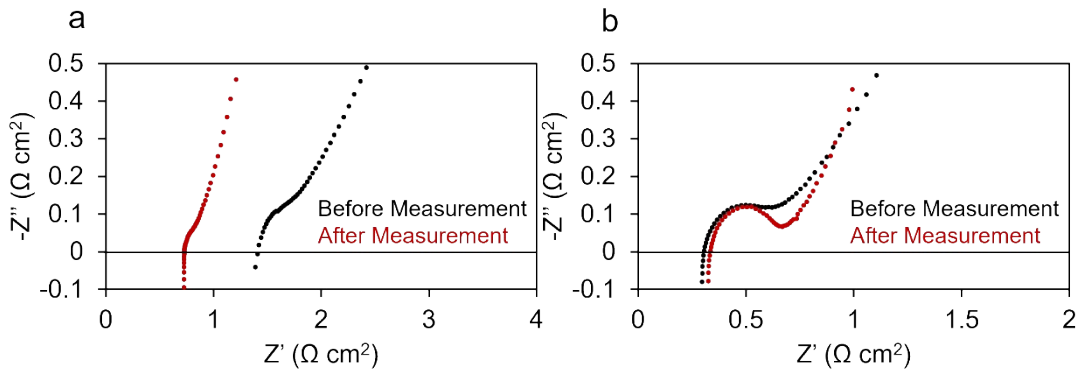

Figure S15. Impedance spectra of MSAGO membranes treated with MSA on (a) the hydrogen-supply side only and (b) the oxygen-supply side only. Black and red dots represent measurements before and after fuel cell operation, respectively.

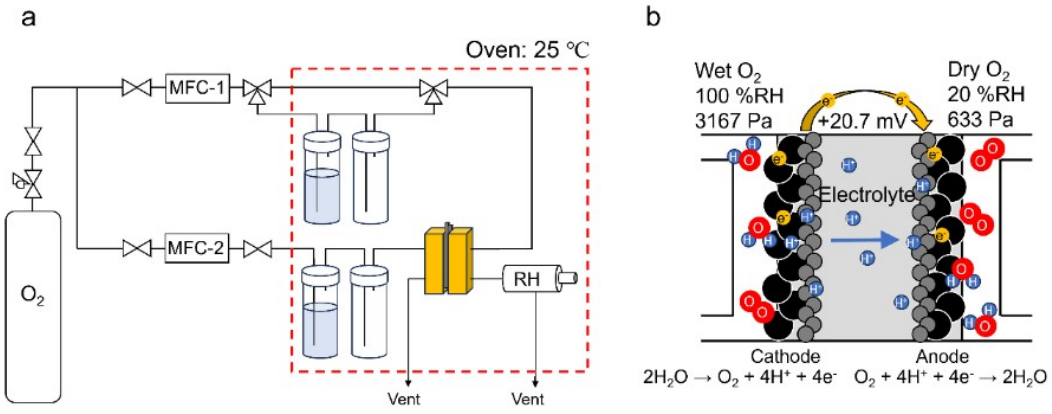

Figure S16. (a) Schematic of the evaluation setup for a concentration-gradient cell using oxygen as the carrier gas. (b) Schematic diagram of reaction in the system of (a).

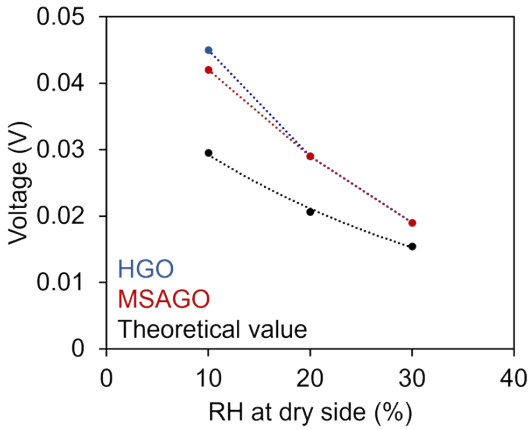

Figure S17. Humidity dependence of the EMF generated by a water vapor concentration gradient in fuel cell using GO and MSAGO membranes as solid electrolytes.

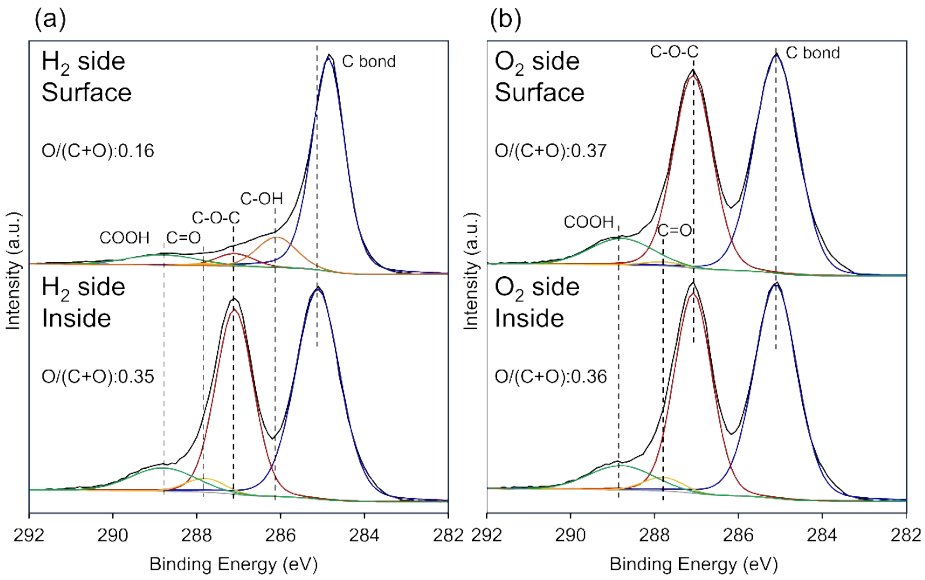

Figure S18. The C 1s XPS spectra of the surfaces and insides of the hydrogen- and oxygen-supply sides of the MSAGO membrane after fuel cell operation.

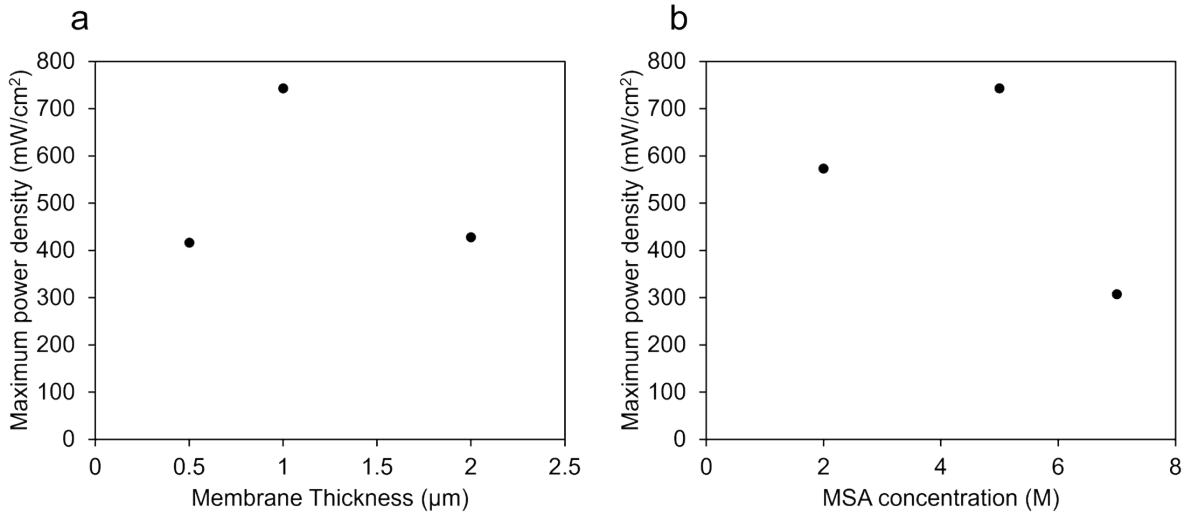

Figure S19. Correlation between maximum power density and (a) MSAGO membrane thickness, (b) maximum power density.

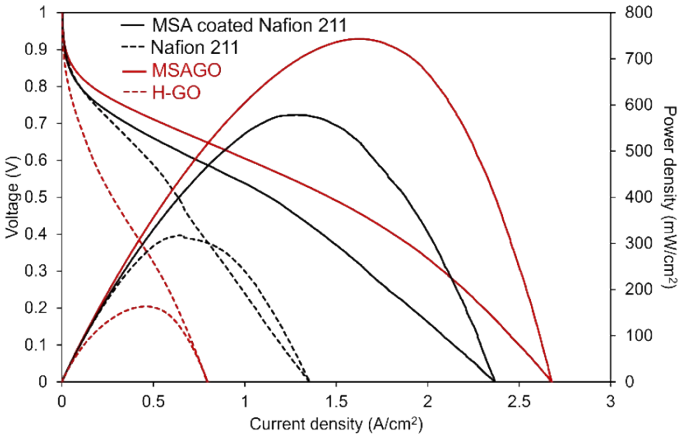

Figure S20. Comparison of fuel cell performance between Nafion 211 membrane (25 μm) and MSAGO membrane (1 μm). The black line represents the Nafion 211 membrane after MSA coating. Dotted lines denote the data obtained before processing, while solid lines denote the data after MSA processing.

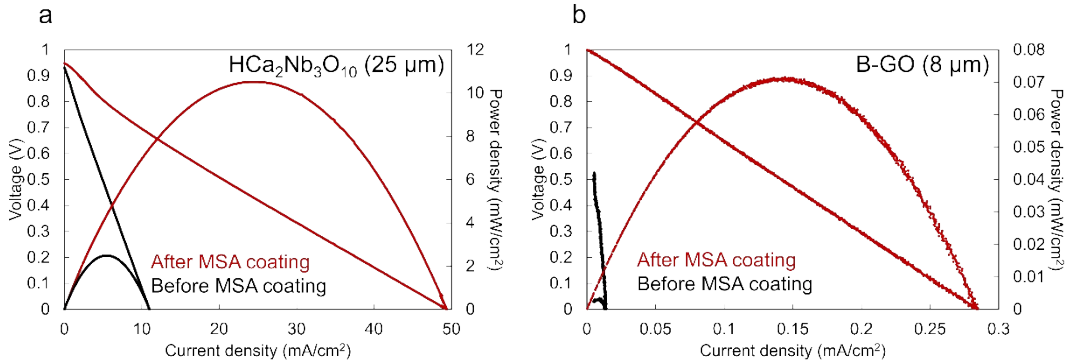

Figure S21. Fuel cell performance using (a) $HCa_2Nb_3O_{10}$ nanosheets as the electrolyte and (b) B-GO membrane as the electrolyte. $HCa_2Nb_3O_{10}$ nanosheets were prepared according to previous reports.[39]

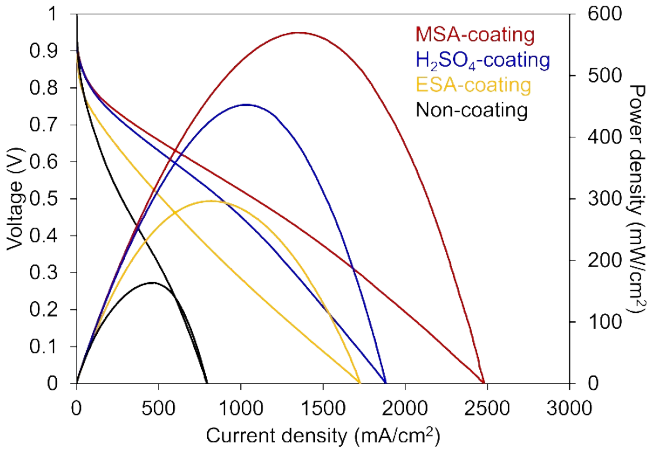

Figure S22. Comparison of acids used for surface coating on H-GO membrane.

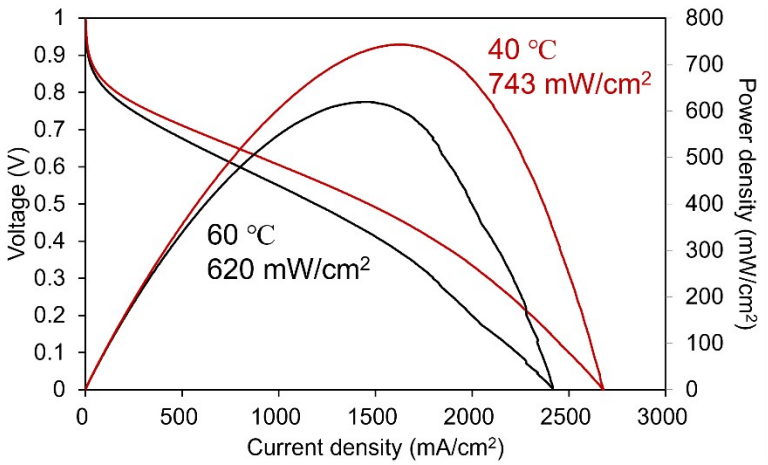

Figure S23. Fuel cell performances of 5 M MSAGO (1 μm) at different temperatures.

Table S1. Summary of the bulk and interfacial resistance values obtained from the fitting of the Nyquist plots shown in Figure S7.

Membrane	Thickness (μm)	MSA concentration (M)	Bulk resistance (Ω)	Interfacial resistance (Ω)
H-GO	2	–	3.91	2.76
MSAGO	2	2	2.24	0.114
MSAGO	2	5	1.21	0.0626

Table R2. Summary of the bulk and interfacial resistance values obtained from the fitting of the Nyquist plots shown in Figure S8.

Membrane	Bulk resistance (Ω)	Interfacial resistance (Ω)
Nafion 211	2.75	1.91
5 M MSA coated Nafion 211	2.21	0.239

Table S3. Comparison of hydrogen permeation rates for Nafion 211, GO, and MSAGO membranes, including their respective thicknesses and reference permeation rate of Nafion211.

Membrane	Thickness(μm)	H_2 gas permeation rate (mL min^{-1} cm^{-2})	Ratio (/Nafion)
Nafion 211	25	1.1×10^{-2}	1
GO	20	4.9×10^{-4}	0.044
MSAGO	20	2.7×10^{-4}	0.024

Table S4. Comparison of temperature, maximum power density, and maximum current density of fuel cells using GO-based electrolytes.

Specimen	Temp.	Maximum power density ($mW\ cm^{-2}$)	Maximum current density ($mA\ cm^{-2}$)	Ref.
Acid-intercalated GO	40	741	2680	This work
GO	30	33.8	>140	25
	40	23.2	>100	
	50	5.5	>20	
	80	0.18	>1	
GO-metal thin film hybrid	60	21	>85	26
	60	3	10	
GO	25	13	50	27
3DGO	30	60.2	300	22
Modified GO	30	136	600	29
	50	184	-	
Acid-intercalation 3DGO	30	113	600	14
Spray-coating GO	30	79	>400	30
Modified GO	40	73.8	442	31
Acid-intercalated 3DGO	30	98.8	400	15
Acid-intercalated GO	80	149	>500	32
3DGO-CNT hybrid	30	117	320	33
Modified GO		2.1	>7	34
Bulk GO	25	80	>500	24
Acid-intercalated 3DGO	30	250	1200	13